

2025 | 457

Evaporation and combustion characteristics study of diesel droplets in premixed ammonia/air

Basic research & advanced engineering - new concepts

Meijia Song, Dalian University of technology

Huazhi Zhao, Dalian university of technology
Mingqiang Liu, Dalian university of technology
Zelong Xie, Dalian university of Technology
Zixin Wang, Dalian university of technology
liyan Feng, Dalian university of technology

This paper has been presented and published at the 31st CIMAC World Congress 2025 in Zürich, Switzerland. The CIMAC Congress is held every three years, each time in a different member country. The Congress program centres around the presentation of Technical Papers on engine research and development, application engineering on the original equipment side and engine operation and maintenance on the end-user side. The themes of the 2025 event included Digitalization & Connectivity for different applications, System Integration & Hybridization, Electrification & Fuel Cells Development, Emission Reduction Technologies, Conventional and New Fuels, Dual Fuel Engines, Lubricants, Product Development of Gas and Diesel Engines, Components & Tribology, Turbochargers, Controls & Automation, Engine Thermodynamics, Simulation Technologies as well as Basic Research & Advanced Engineering. The copyright of this paper is with CIMAC. For further information please visit <https://www.cimac.com>.

ABSTRACT

To effectively utilize ammonia as a carbon-free fuel in engines, one solution is to use diesel as a highly reactive fuel to ignite the ammonia. In a diesel-ammonia dual-fuel engine with diesel direct injection, the evaporation, breakup, and combustion characteristics of the diesel spray in the ammonia atmosphere are key issues. Studying the fundamental physicochemical properties of single droplet evaporation and combustion is the basis for spray research.

Therefore, this study conducted experimental research on the evaporation and auto-ignition behavior of single diesel droplets in premixed ammonia/air mixtures in a visual rapid compression machine (RCM). Single diesel droplets (40-250 μm) were suspended at the center of the combustion chamber using a fiber. The experimental conditions were temperature of 700-950K and pressure of 12-32 bar. The equivalence ratio of ammonia ranged from 0 to 1.0. High-speed cameras with long and short focus lenses were used to capture the changes in droplet diameter and flame generation.

The results showed that the evaporation rate of droplets increased with increasing temperature. Due to the high thermal conductivity of ammonia, the evaporation rate of droplets in $\text{NH}_3/\text{Ar}/\text{N}_2$ gas was higher than in Ar/N_2 gas. The addition of ammonia gas shortens the heating and evaporation durations, leading to a reduction in the droplet lifetime. In addition, the ignition delay times (IDTs) of diesel droplets increased with droplet diameter and decreased with increasing temperature and pressure. The IDTs of droplets in ammonia are higher than that in air and increases with the increase of equivalence ratio. However, the effect of ammonia increasing IDT became less significant when the equivalent ratio increases. This is the result of the dual effect of promoting evaporation and inhibiting combustion by ammonia.

At the same time, the experiment captured the ellipse flame front of diesel droplets at the ignition moment, with the ignition radius decreasing with increasing pressure, while increasing with the higher ammonia content in the background gas due to the lower viscosity of ammonia. When ammonia is burned, as the equivalence ratio and temperature increase, the maximum pressure rise rate and the heat release rate increase, while the combustion duration becomes shorter. The maximum pressure rise rate increases exponentially with the increase in the equivalence ratio. As pressure increases, the maximum pressure rise rate and the heat release rate increase, but the combustion duration becomes longer.

1 INTRODUCTION

To reduce greenhouse gas emissions from the shipping industry, the International Maritime Organization (IMO) adopted the 'IMO Strategy on Reduction of GHG Emissions from Ships' in 2023, which establishes a target to reduce the carbon intensity of shipping emissions by 40% relative to 2008 levels by 2030, and aims to achieve net-zero greenhouse gas emissions from international shipping by 2050 [1]. To reach these goals, the development of low-carbon and zero-carbon fuel engines has become a necessary pathway [2,3]. In recent years, ammonia has emerged as the preferred zero-carbon fuel for marine engines due to its advantages, including ease of liquefaction (at -33°C under normal pressure, or 0.9 MPa at ambient temperature), ease of storage and transportation (using standard liquefied gas cylinders), and good explosion resistance [4,5]. However, ammonia also presents several disadvantages, including a high auto-ignition temperature (924K, compared to 527K for diesel), low calorific value, low flame speed (7 cm/s, compared to 291 cm/s for hydrogen and 37 cm/s for methane), and high ignition energy, which may lead to issues such as ignition misfire, low combustion efficiency, and increased emissions [6].

To enable the effective use of ammonia in compression ignition engines, the ammonia-diesel dual-fuel combustion mode has been widely studied in recent years through both experiments and simulations [7-9]. This mode is typically classified into two types: high-pressure direct injection ammonia diffusion combustion and Low-pressure early injection ammonia premixed combustion [10-14]. In the ammonia premixed combustion mode, a small amount of pilot diesel is injected as a highly reactive fuel to ignite the ammonia-air mixture. Since fuel combustion performance is critical to engine efficiency, understanding the combustion and flame propagation characteristics of pilot diesel in ammonia is crucial for enhancing engine performance and reducing harmful emissions.

The auto-ignition and combustion of the pilot diesel directly affects the subsequent combustion process. Investigating the evaporation characteristics of diesel droplets is crucial for understanding spray dynamics and combustion [15]. As a result, extensive research has been conducted by numerous scholars on the evaporation and combustion of single liquid droplets. Many experimental and simulation studies have focused on the combustion of single droplets of diesel and diesel alternative fuels. These studies primarily examine the effects of environmental thermodynamic conditions and droplet composition

on the evaporation and auto-ignition characteristics of the droplets. In 2014, Kim et al. [16, 17] studied the evaporation and auto-ignition characteristics of a single n-heptane droplet in a rapid compression machine. The results showed that under the varying temperature and pressure conditions in the rapid compression machine, the droplet diameter decreased with changes in the evaporation rate. The evaporation rate of the droplet increased with larger droplet diameters and higher temperatures. The larger the initial droplet diameter, the slower the droplet heating rate, resulting in a longer ignition delay time. In 2015, Hashimoto et al. [18] measured the evaporation process of droplets of n-hexadecane, diesel, and palm methyl ester (PME), comparing the results of PME with those of diesel and n-hexadecane. The study found that the droplet lifetime of PME is longer than that of diesel fuel and n-hexadecane at the same ambient temperature. In 2023, Pang et al. [19] used ultrasonic levitation to study the evaporation behaviour of n-hexadecane and diesel droplets. The results indicated a positive correlation between evaporation rate and temperature, with significant differences in the evaporation rates between n-hexadecane and diesel droplets. In 2022, Ju et al. [20] conducted an experimental visualization study on the evaporation rate constants of a single diesel fuel droplet in subcritical and supercritical environments and performed molecular dynamics simulations. The results showed that in supercritical conditions, the D^2 law was no longer strictly applied and the evaporation rate constant became a variable with increasing evaporation time.

In practical engines, diesel fuel droplets are surrounded by various gases. However, research on the influence of background gas composition on the evaporation and combustion of hydrocarbon droplets is limited. In 2014, Yi Ping et al. [21] developed an improved multi-component diesel evaporation model, which included an enhanced enthalpy diffusion model, a corrected Stefan velocity, and time-varying thermophysical properties. The model was validated using experimental data. And the effects of O_2 , CO_2 and EGR concentration on the fuel droplet vaporization rate were studied under different environmental temperature and pressure conditions. In 2018, Markadeh et al. [22] developed a discrete multi-component (DMC) model for droplet evaporation in convective environments. The study investigated the evaporation process of diesel droplets under different environmental conditions and compositions. The results showed that, in an $\text{N}_2\text{-O}_2$ mixed environment, as the oxygen mass fraction increased from 0 to 1, the droplet lifetime first decreased and then increased. EGR caused slight

changes in droplet lifetime and heating period. In 2022, Siddique et al. [23] conducted evaporation and combustion experiments of individual diesel droplets in methane within a rapid compression machine (RCM). Several auto-ignition modes were observed near the droplet. The ignition delay time of oil droplets increases with the increase of the equivalence ratio of ambient gas. A transient analysis droplet evaporation model was developed using CONVERGETM, which predicted the ignition delay time (IDT) of the droplets accurately. In 2022, Wang et al. [24] studied the auto-ignition behaviour of cylinder oil droplets in a methane atmosphere within an RCM. The results showed that the effect of methane on the overall ignition delay of the droplet depended on the initial droplet diameter. In 2024, Wang et al. [25] studied the effects of EGR gases (specifically CO₂ and H₂O) on gas-fuel premixed ignition in an RCM. The results indicated that EGR played a crucial role in increasing the ignition delay time of droplets and thus postponing the occurrence of pre-ignition. Additionally, EGR could reduce the flame propagation speed, thus decreasing the maximum combustion pressure.

Generally, research on the influence of background gas composition on the evaporation and combustion of hydrocarbon fuel droplets has primarily focused on gases such as EGR gases and methane. However, there has been limited research on the evaporation and auto-ignition of diesel droplets in an ammonia-rich environment, and the impact of ammonia on diesel droplet evaporation and auto-ignition remains unclear.

Therefore, this study employs an optical Rapid Compression Machine to investigate the evaporation and auto-ignition of diesel droplets in

an ammonia-rich gas environment. The effects of droplet size, temperature, pressure, and the equivalence ratio of the ambient gas on the droplet ignition delay time, droplet ignition radius, ammonia-air mixture combustion duration, and maximum pressure rising rate were examined. Additionally, the impact of ammonia in the ambient gas on diesel droplet evaporation was explored. The results provide valuable insights for the development of ammonia-diesel combustion numerical models and the design of ammonia-diesel dual-fuel engines.

2 MATERIAL AND METHODS

2.1 Experimental setup

The evaporation and auto-ignition processes of a single droplet and flame propagation of ammonia-air pre-mixture were investigated using an optical Rapid Compression Machine developed by Dalian University of Technology. The RCM, driven by gas and mechanically braked, simulates a similar adiabatic compression process to replicate the high temperature and pressure conditions typical of an engine. The compression process lasts approximately 25 ms, and the combustion chamber has an inner diameter of 50.8 mm. The experimental setup is shown in Figure 1, with detailed parameters provided in reference [26].

Micro-droplet generators were used to produce diesel droplets of various sizes, which were then suspended on fibers (with a fiber diameter of 0.015 mm and a length of approximately 4-6 mm). The droplets were positioned at the center of the chamber. The experiments used China National Standard No. 0 Diesel, with its physical and chemical properties listed in Table 1.

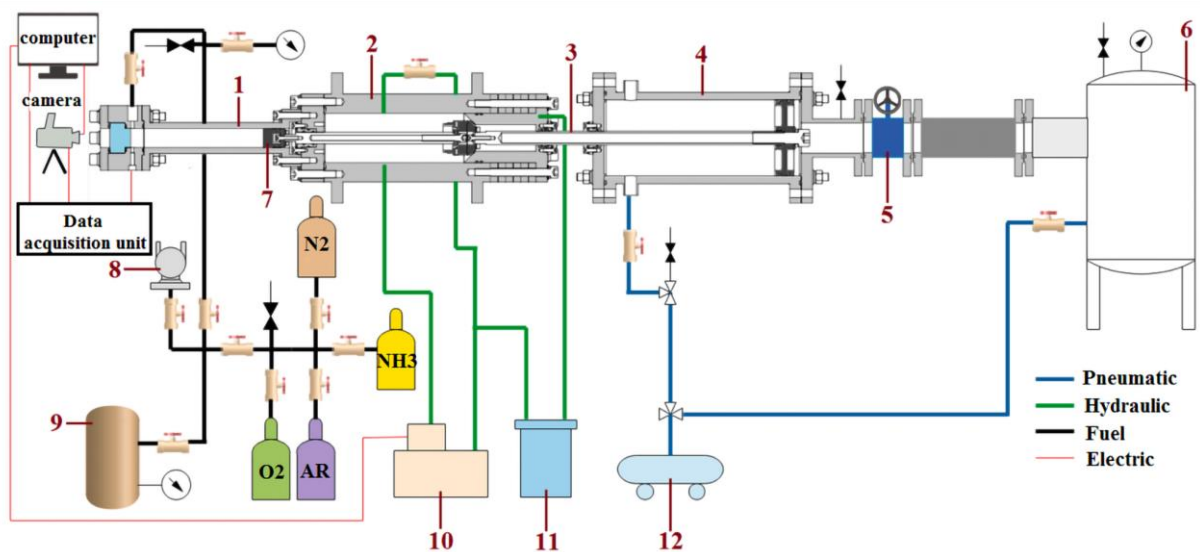


Figure 1. Schematic of RCM. (1: Combustion chamber, 2: Hydraulic cylinder, 3: Connecting rod, 4: Driving cylinder, 5: Motor switch, 6: High-pressure tank, 7: Combustion piston, 8: vacuum pump, 9: Mixing tank, 10: Hydraulic pump, 11: Storage barrel, 12: Air compressor). (Incomplete schematic of optical path)

For practical reasons, the droplet size range in the experiments was from 40 to 250 μm . Two high-speed cameras were used during the experiments. During the droplet evaporation experiments, a long-focus camera positioned opposite the observation window was used to record the changes in droplet diameter under parallel lighting conditions. The two symmetrical spotlights provide light to the chamber.

Table 1. Physical and chemical properties of GB No. 0 Diesel [27].

Parameter	Value
Density (293K) (g/cm^3)	0.84-0.86
Kinematic viscosity (mm^2/s)	3.0-8.0
Heating value (MJ/kg)	42-46
freezing point (K)	258.15~263.15
Sulfur concentration	<0.2%
Cetane number	≥ 40

In the auto-ignition experiments, both a high-speed camera with a 105 mm lens and a long-focus camera were used. Initially, the long-focus camera captured the droplet's initial diameter under high-light conditions, before the compression stroke. As the compression stroke began, the high-speed camera operating under low-light conditions (to ensure clear imaging) recorded the auto-ignition of the diesel droplet and the subsequent flame propagation of the ammonia-premixed gas. The optical measurement setup is shown in Figure 2.

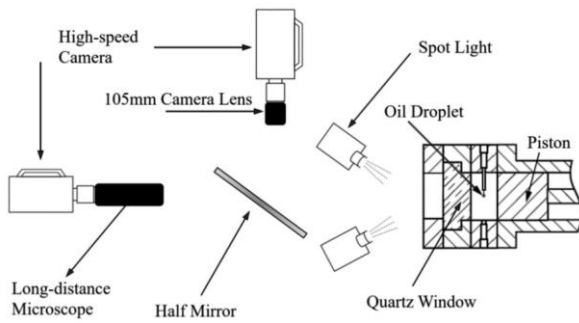


Figure 2. The schematic of the dual high-speed camera optical system.

2.2 Data processing of optical images.

The magnified droplet images captured by the long-focus camera were processed using MATLAB code to determine the droplet diameter. The image processing procedure is shown in Figure 3. First, the required region of interest was extracted. The image was then binarized to obtain a binary image. After that, fibers in the image were removed, and the irregular boundaries of the image were optimized. The actual length was calculated by determining the number of pixels per unit length. Finally, the droplet diameter was determined using

a volume conversion approach. Specifically, it was assumed that the droplet diameter along the fiber direction was the same, and the volume of the ellipsoid was converted to the volume of a sphere with the same volume. The diameter of this sphere was defined as the initial droplet diameter (D_0).

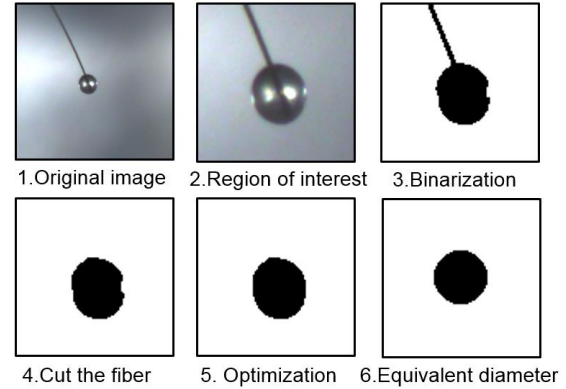


Figure 3. Image processing of oil droplet diameter.

In the experiment, diesel initially auto-ignited under high temperature and pressure, which then ignited the surrounding ammonia, resulting in a flame propagating outward. The macroscopic flame shape can be estimated based on the assumption of a spherical flame [28]. This image was also processed using a MATLAB program. The ratio of the flame area to the RCM visible window area (with a diameter of 50.8 mm) at different times reflects the flame propagation speed.

2.3 Testing Conditions and mixture preparation

In the experiment, the cylinder pressure was recorded using a pressure transducer (AVL GH14DK) in the combustion cylinder, with a charge amplifier (AVL 2P2x), and an NI acquisition device (CRIO-9042) to process the pressure signal into available data. The initial temperature and pressure are denoted as T_0 and P_0 . The temperature and pressure at the end of compression (or called top dead center TDC) are referred to as the compression temperature (T_c) and compression pressure (P_c). The T_c , which cannot be measured directly, is determined based on the "adiabatic core" hypothesis [29]:

$$\int_{T_0}^{T_c} \frac{\gamma(T)}{\gamma(T)-1} \frac{dT}{T} = \ln\left(\frac{P_c}{P_0}\right) \quad (1)$$

where $\gamma(T)$ is the specific heat ratio of the reactant mixture and is temperature dependent.

Figure 4 shows the typical in-cylinder pressure curves and pressure derivative curves measured under different conditions. As shown, the time

when the high-speed camera captures the first frame of flame luminosity corresponds to the onset of droplet auto-ignition, with the ignition times defined as t_{ign} . The ignition delay time (IDT) is defined as the time interval between the end of compression (t_0), as derived from the pressure curve, and the auto-ignition time (t_{ign}) of the diesel droplet captured by the high-speed camera. The red curve ($\text{NH}_3/\text{O}_2/\text{AR}$ with oil) represents the in-cylinder pressure curve for the combustion of the ammonia-air mixture with an equivalence ratio of 0.5 initiated by the auto-ignition of a $150\text{ }\mu\text{m}$ diesel droplet under conditions of $T_c=820\text{K}$, $P_c=22\text{ bar}$. IDT1 refers to the ignition delay time (from t_0 to $t_{\text{ign}1}$) under this operating condition. In red curve, a pressure rise due to flame propagation is observed, and the time interval between droplet auto-ignition and the maximum pressure (which corresponds to nearly complete combustion of the cylinder gas and serves as a reference) is defined as the combustion duration, reflecting the burning time. The blue line represents the time derivative of the pressure curve, reflecting the rate of pressure increase during combustion. The green curve corresponds to the in-cylinder pressure change in the absence of fuel droplets under the same operating conditions of the red curve, where no compression occurs. The black curve (O_2/AR with oil) shows the in-cylinder pressure for the auto-ignition of a $150\text{ }\mu\text{m}$ diesel droplet in the air under conditions of $T_c=820\text{K}$, $P_c=22\text{ bar}$, where no significant pressure rise is observed. IDT2 refers to the ignition delay time (from t_0 to $t_{\text{ign}2}$) under this operating condition. The purple curve represents the in-cylinder pressure during a pure evaporation experiment of diesel droplets in an oxygen-free environment under the same operating conditions of the black curve, which nearly overlaps with the black and green curves, indirectly verifying the repeatability of the cylinder pressure measurements.

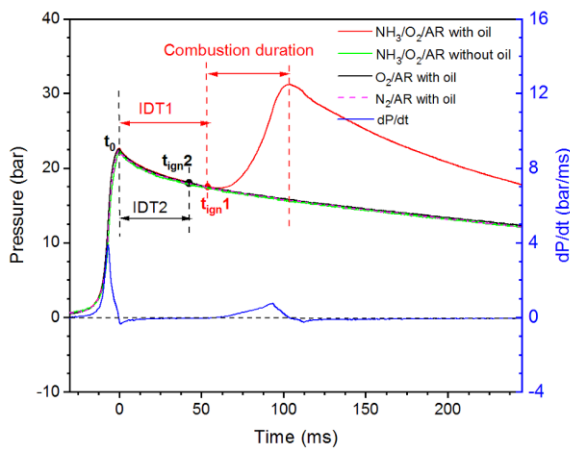


Figure 4. Typical pressure curves and pressure derivative curves under several different conditions.

The preparation of the mixture is described in reference [12]. Table 2 presents the specific composition of the mixtures and thermodynamic conditions for the auto-ignition experiments. A total of five different mixtures were tested. To achieve higher temperatures, argon was used as a substitute for nitrogen. The argon-to-oxygen molar ratio maintained at 3.76, which is the same as in air. The equivalence ratio (ϕ) of the mixture is defined as the ratio of the actual fuel-to-oxygen ratio to the stoichiometric fuel-to-oxygen ratio.

Table 2. Mixture compositions in the auto-ignition experiments.

Mixture	ϕ	Components
1	0	$\text{O}_2/\text{AR}=0.21/0.79$
2	0.5	$\text{NH}_3/\text{O}_2/\text{AR}=0.123/0.184/0.693$
3	0.6	$\text{NH}_3/\text{O}_2/\text{AR}=0.144/0.180/0.676$
4	0.8	$\text{NH}_3/\text{O}_2/\text{AR}=0.183/0.172/0.645$
5	1.0	$\text{NH}_3/\text{O}_2/\text{AR}=0.219/0.164/0.617$

Table 3. Mixture compositions in the evaporation experiments.

Mixture	Components
1	$\text{N}_2/\text{AR}=0.21/0.79$
2	$\text{NH}_3/\text{N}_2/\text{AR}=0.219/0.164/0.617$

Table 3 shows the specific composition of the mixtures in the evaporation experiments. To ensure consistency with the combustion experiments, the O_2 in the mixtures with equivalence ratios of 0 and 1 was replaced with an equivalent amount of N_2 for the evaporation experiments, serving as a control. Additionally, a control experiment was conducted to investigate the effect of adding ammonia to N_2 .

3 RESULTS AND DISCUSSION

3.1 Evaporation and auto-ignition of diesel oil droplets in O_2/AR

The evaporation and combustion experiments of diesel droplets were first conducted in O_2/AR mixture. The range of droplet diameters in this experiment varied from 40 to $250\text{ }\mu\text{m}$. Figure 5 shows the auto-ignition images of diesel droplets of different initial diameters under the conditions of $P_c = 820\text{K}$ and $T_c = 22\text{ bar}$, captured using the short-focus lens (150 mm) in low light conditions. It can be observed that the combustion of the droplets presents a bright white-orange light. The IDT of the droplet gradually lengthens and the flame brightness increases as the droplet diameter increases. Among these, Figure 5d shows the flame image corresponding to a $120\text{ }\mu\text{m}$ diameter droplet captured by the long-focus lens (with a shooting frequency of 5000 fps). As the oil vapor spreads outward and reaches a certain concentration, ignition occurs, forming an elliptical

flame front away from the droplet surface. The distance along the vertical fiber direction of the flame front is defined as the ignition radius, with an ignition time error of less than 0.2 ms. At this moment, a pressure wave propagating rapidly outward from the droplet center was simultaneously captured. It is indicated by a blue dashed line since it is difficult to distinguish in the image. The heat generated by the combustion then causes the droplet to evaporate rapidly, and the resulting oil vapor continues to burn.

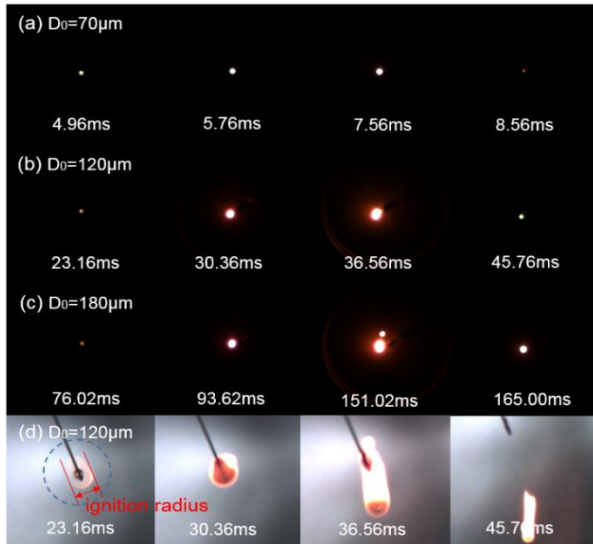


Figure 5. Visual images of the combustion process of diesel droplets of different diameters in O_2/AR . ($P_c = 820\text{K}$, $T_c = 22\text{ bar}$) (time after the TDC). Panels (a), (b), and (c) were captured with a short-focus lens, while panel (d) was captured with a long-focus lens.

Figure 6 presents the IDTs of diesel droplets of different initial diameters at different temperatures in the air. It can be observed that the IDT of the droplet increases as the initial diameter of the droplet increases at the same temperatures. The increase in droplet diameter results in a decrease in the surface-to-volume ratio of the droplet, meaning that heat transfer takes longer. This leads to a longer time required for the droplet to heat up and evaporate, thus increasing the ignition delay time. As the temperature increases, the IDT tends to decrease. However, between 875K and 950K, the decrease becomes less significant.

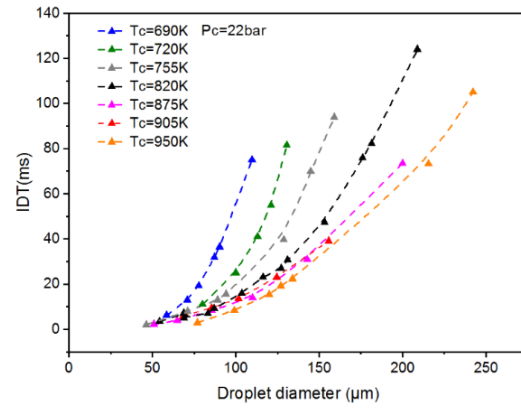


Figure 6. IDTs of diesel droplets of different diameters under different temperature conditions in O_2/AR . ($P_c = 22\text{ bar}$).

Figure 7 shows the IDTs of diesel droplets of different initial diameters at different pressures. It can be observed that the IDT of the droplets increases significantly as the pressure falls below 22 bar. Especially under the 12 bar condition, auto-ignition becomes more difficult. The IDT remains almost unchanged as the pressure increases above 22 bar. According to previous studies, the trend of droplet evaporation rate with pressure variation is temperature-dependent [31]. The evaporation experiment results in Section 3.3 show that under the 12–32 bar conditions, the evaporation rate of droplets of the same size changes little in the O_2/AR mixture. Therefore, the IDT is primarily influenced by the chemical ignition delay time. Within this pressure range, further increasing the pressure gradually weakens its promoting effect on combustion, resulting in little change in ignition delay. However, at lower pressures, the chemical ignition delay time of the droplets is longer and the temperature and pressure inside the cylinder also decrease more significantly, leading to a considerable increase in the overall IDT.

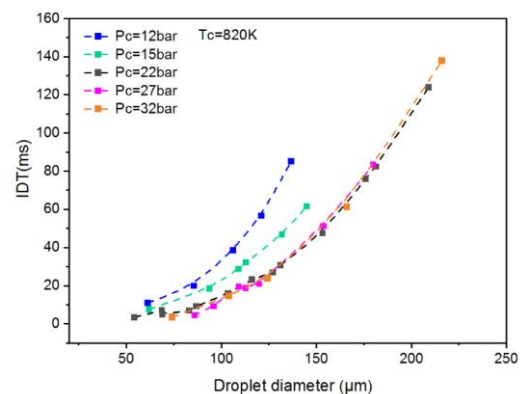


Figure 7. IDTs of diesel droplets of different diameters under different pressure conditions in O_2/AR . ($T_c=820\text{K}$)

3.2 The auto-ignition of diesel droplets and flame propagation in ammonia-air mixtures

3.2.1 Effect of droplet diameter and mixture equivalent ratio

The IDTs of diesel droplets were measured in ammonia-air mixtures with different equivalence ratios. As shown in Figure 8, the IDTs of diesel droplets in ammonia-air mixtures were measured at $P_c = 22$ bar and $T_c = 820$ K. It can be observed that the IDTs of diesel droplets in ammonia are higher than in air. For the $150\text{ }\mu\text{m}$ droplet, the IDT in the ammonia-air mixture with an equivalence ratio of 0.5 is approximately 1.5 times that in air, while the IDT in the mixture with an equivalence ratio of 1.0 is about twice that in air. As the equivalence ratio increases, the rate of IDT increase diminishes. The IDT values in mixtures with equivalence ratios of 0.8 and 1.0 are almost identical. This behavior can be explained by the fact that the ignition delay time of diesel droplets is the result of both chemical and physical ignition delays [24]. According to the evaporation experiment results from Section 3.3, it is known that the addition of ammonia promotes the evaporation of diesel droplets. As the ammonia content increases, the combined effects of promoting evaporation and inhibiting combustion leading to the observed results.

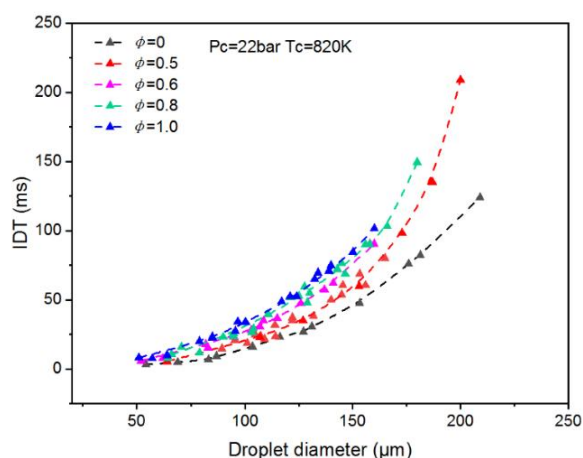


Figure 8. IDTs of diesel oil droplets of different initial diameters in ammonia-air mixture with different equivalent ratios ($T_c=820$ K, $P_c=22$ bar).

Similarly, the IDT of diesel droplets increases with droplet diameter under different equivalence ratios. Figure 9 shows the cylinder pressure traces and pressure derivative curves for ammonia-air mixture ignited by diesel droplets of various sizes in a mixture with an equivalence ratio of 0.5. It can be observed that the combustion pressure rising rates are nearly identical across all curves. However, as the IDT of the droplets increases, both the in-cylinder temperature and pressure decrease,

leading to a slight reduction in peak pressure and a slight increase in the duration of combustion.

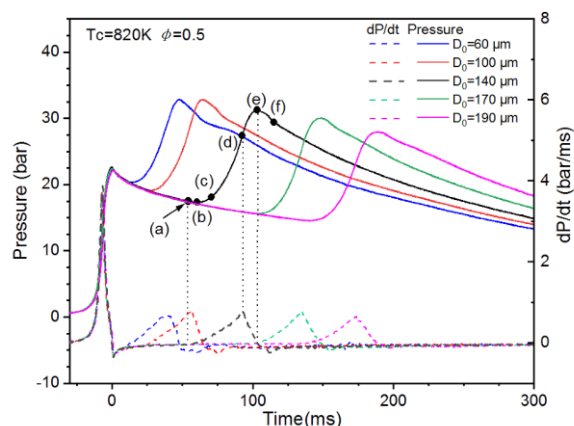


Figure 9. The pressure curves of ammonia-air mixture (with equivalence ratio of 0.5) ignited by diesel droplets of various initial diameters in a mixture. ($T_c=820$ K, $P_c=22$ bar).

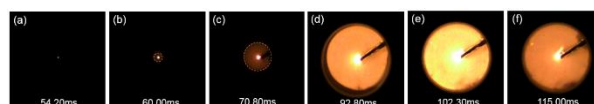


Figure 10. Flame images of ammonia-air mixture (with equivalence ratio of 0.5) ignited by a $140\text{ }\mu\text{m}$ diesel droplet. (Corresponds to Figure 9.)

Figure 10 shows the flame propagation images of the ammonia-premixed gas ignited by $140\text{ }\mu\text{m}$ diesel droplets corresponding to each stage depicted in Figure 9. The recording frequency is 10,000 fps. As can be seen, 54.2 ms after the top dead center (ATDC) (point (a)), the oil vapor evaporated around the oil droplet is first auto-ignited, forming a flame. Then the surrounding ammonia gas was ignited and the downward trend of the pressure curve changed. At 60 ms ATDC (point (b)), a faint orange ammonia flame is visibly formed around the oil droplet, with the flame front clearly exhibiting a relatively regular spherical shape (indicated by the orange dashed line in the figure). The spherical flame continues to propagate outward, and the pressure curve gradually bends upward. Due to the combustion chamber's cylindrical shape, with a height smaller than its diameter, when the flame reaches the front and rear bottom surfaces of the chamber, it continues to propagate in the circumferential direction. The brightness gradually increases, and the flame front becomes more pronounced. At point (d), the pressure rising rate reaches its maximum. Then, at point (e), the bright yellow flame fills the entire circular window, and the pressure reaches its peak. Afterwards, the pressure decreases, and the flame

brightness diminishes. By point (f), the gas within the cylinder has been completely combusted.

Figure 11 shows the combustion images of ammonia-air mixture with different equivalence ratios ignited by diesel droplets with an initial diameter of 125 μm in mixtures under the conditions of Figure 8. The six time points and corresponding images are aligned with the six defined points in Figure 9. It can be observed that the overall brightness of the flame intensifies as the equivalence ratio increases. In the image at an equivalence ratio of 1, a pink color appears in the middle phase of the flame, which may be related to the radiation of light at specific wavelengths by certain molecules at high temperatures during the combustion process.

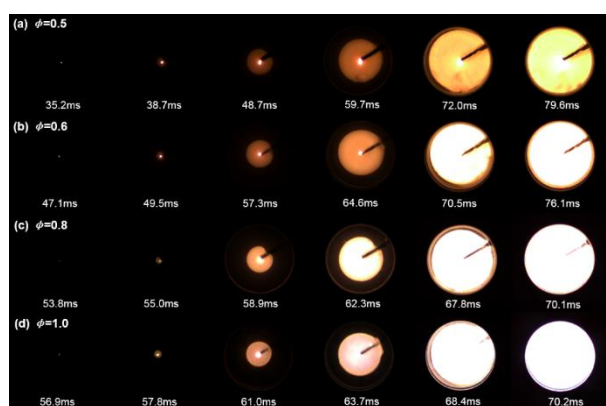


Figure 11. Flame images of ammonia-air mixture with different equivalence ratios ignited by a 125 μm diesel droplet ($T_c=820\text{K}$, $P_c=22\text{ bar}$).

Figure 12 shows the in-cylinder pressure curves and pressure derivative curves for the four experimental conditions. The pressure derivative values serve as an important indicator of the heat release rate (HRR), which can be used to assess the magnitude of HRR [32]. The position of the dots in the figure indicates the ignition time. It can be observed that the IDT of the droplets increases as the equivalence ratio increases. The maximum pressure rising rate, heat release rate, and peak pressure all increase during ammonia combustion. The maximum pressure rising rates for gases with equivalence ratios of 1, 0.8, and 0.6 are 11.7, 5.27, and 2 times greater than that for the gas with equivalence ratio of 0.5, respectively. As the equivalence ratio increases, the maximum pressure rising rate increases approximately exponentially. Additionally, for the experimental groups with equivalence ratios of 0.5, 0.6, and 0.8, the times at which the maximum pressure rising rate and peak pressure occur decrease as the equivalence ratio increases.

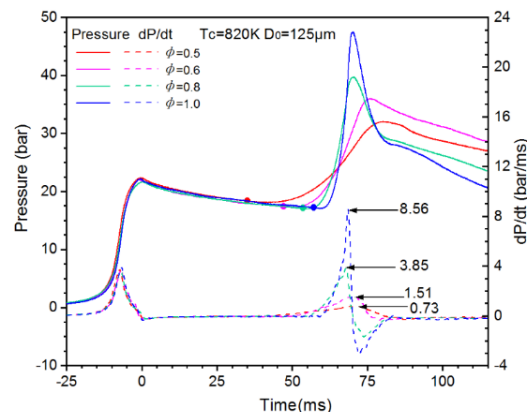


Figure 12. Pressure curves and pressure derivative curves of ammonia-air mixture ignited by diesel droplets under different equivalence ratio conditions (corresponding to Figure 11).

Figure 13 shows the relative flame area calculated for the four experimental conditions, which reflects the flame propagation speed. It can be observed that the flame propagation speed is initially slow during the early flame development stage, then accelerates, and slightly slows down before the relative flame area approaches 1. Overall, the flame propagation speed increases significantly with the increase in the equivalence ratio.

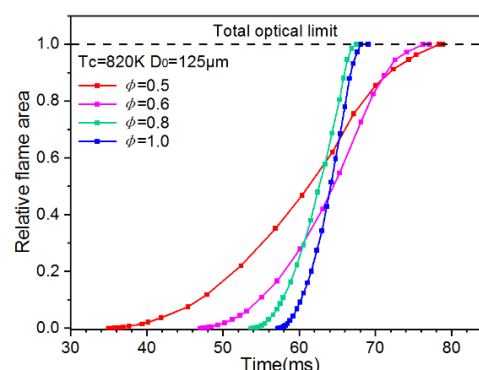


Figure 13. Relative flame area of ammonia-air mixture ignited by diesel droplets under different equivalence ratio conditions (corresponding to Figure 11).

3.2.2 Effect of temperature

To investigate the effect of temperature on the auto-ignition of fuel droplets and the flame propagation of ammonia, the ignition delay time of the droplets and flame propagation characteristics were studied by varying the temperature (T_c) under different equivalence ratio conditions. It can be observed in Figure 14 that the IDT of the fuel droplets decreases with increasing temperature. Under an equivalence ratio of 0.5, the IDT of 150 μm droplets at 755 K is approximately 1.5 times greater than that at 820 K, while the IDT of 150 μm

droplets at 885 K is about 0.5 times that at 820 K. Similar trends are observed under other equivalence ratio conditions. Figure 15 shows the combustion images of ammonia-air mixture with equivalence ratio of 0.5 ignited by diesel droplets with an initial diameter of 140 μm in a 0.5 equivalence ratio mixture, under the conditions of Figure 14. It can be observed that the flame brightness at each stage increases as the temperature rises. As the temperature increases, the evaporation rate accelerates, leading to a reduction in both the chemical and physical ignition delay times.

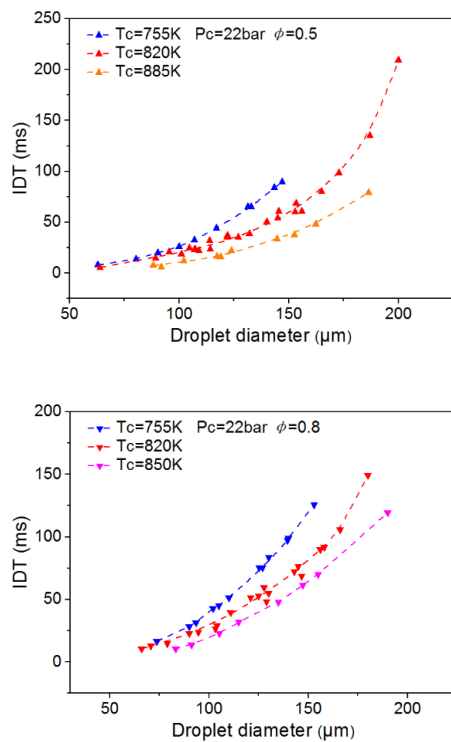


Figure 14. IDTs of diesel oil droplets of different initial diameters in ammonia-air mixture with different equivalent ratios under different temperature conditions ($P_c=22$ bar) .

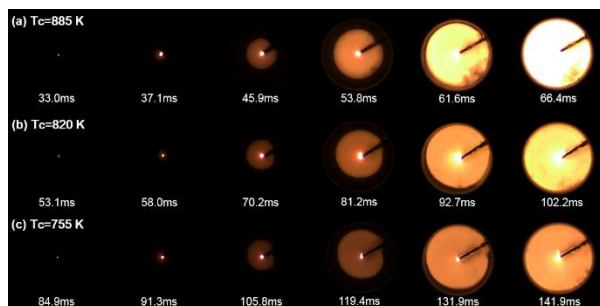


Figure 15. Flame images of ammonia-air mixture (with equivalence ratio of 0.5) ignited by a 140 μm diesel droplet under different temperature conditions ($P_c=22$ bar) .

Figure 16 presents the corresponding pressure and pressure derivative curves for the combustion images. It can be seen that the chemical reaction rate accelerates as the temperature increases, resulting in a larger maximum pressure rising rate during ammonia combustion. In addition, the heat release rate increases and the combustion duration shortens with the increase in temperature. At 885 K, the maximum pressure rising rate is approximately 1.36 times that at 820 K, with the increase being smaller compared to the effect of the equivalence ratio. Figure 17 shows the corresponding plot of the relative flame area. It can be inferred that the flame speed slightly increases as the temperature increases. This is because an increase in temperature raises the kinetic energy of the reactant molecules, which promotes the diffusion of heat and reactants. Additionally, the rate of chemical reactions increases with temperature, ultimately leading to faster flame propagation.

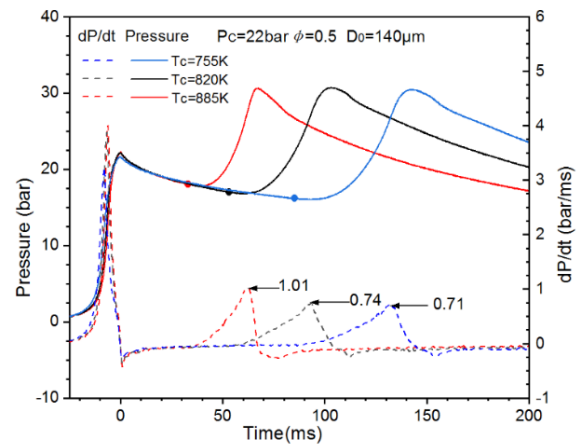


Figure 16. Pressure curves and pressure derivative curves of ammonia-air mixture ignited by diesel droplets under different temperature conditions.

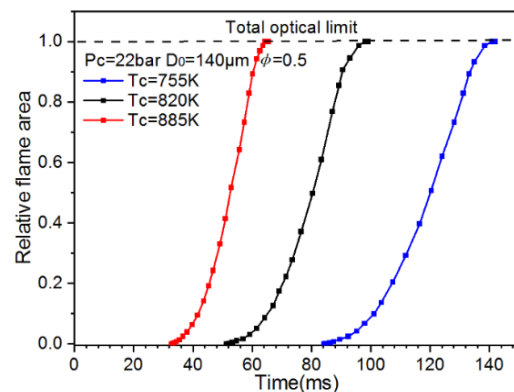


Figure 17. Relative flame area of ammonia-air mixture ignited by diesel droplets under different temperature conditions (corresponding to Figure 15).

3.2.3 Effect of pressure

To investigate the effect of pressure on the ignition delay time and flame propagation of oil droplets, experiments were conducted at different equivalence ratios of ambient gases with varying pressures. As shown in Figure 18, the results indicate that the IDT of oil droplets decreases with increasing pressure across all equivalence ratios at $T_c = 820K$. However, the variation pattern differs slightly for different equivalence ratios. At an equivalence ratio of 0, the IDT at 32bar is nearly identical to that at 22bar. As the equivalence ratio increases, the difference in IDTs between the 32bar and 22bar conditions gradually becomes more pronounced. According to the evaporation experiment results in Section 3.3, the droplet life decreases significantly and the evaporation rate increases markedly under the condition of 32bar in ammonia-air environment compared with air environment. Therefore, the oil droplet evaporates more rapidly under conditions with a higher ammonia content, leading to a shorter physical ignition delay.

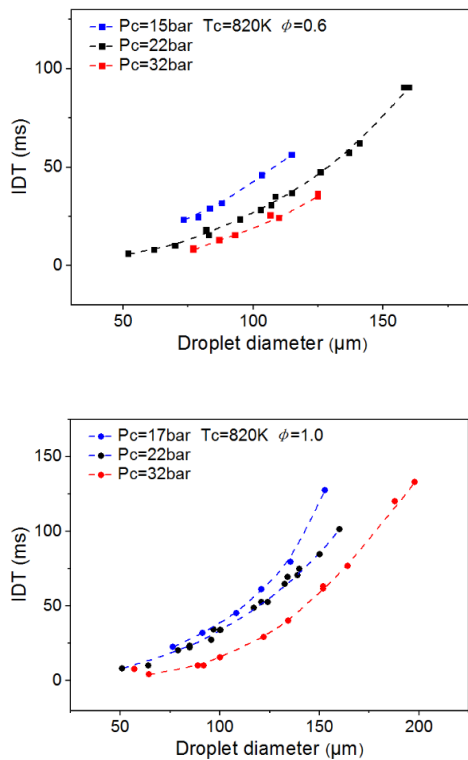


Figure 18. IDTs of diesel oil droplets of different initial diameters in ammonia-air mixture with different equivalent ratios under different pressure conditions ($T_c=820K$).

Figure 19 shows the combustion images of ammonia-air mixture with equivalence ratio of 0.6 ignited by diesel droplets with an initial diameter of 90 μm under the conditions shown in Figure 18. It

can be observed that the flame brightness at all stages increases with the rise in pressure. This is due to the increased heat release density during the combustion process at higher pressures, which results in stronger radiation and thus enhances the flame brightness.

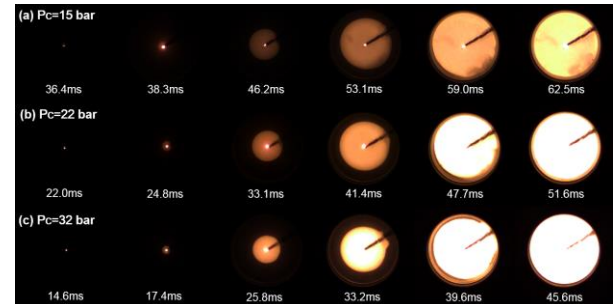


Figure 19. Flame images of ammonia-air mixture (with equivalence ratio of 0.6) ignited by a 90 μm diesel droplet under different pressure conditions ($T_c=820K$).

Figure 20 presents the corresponding pressure and pressure derivative curves for the combustion images. It can be observed that the maximum pressure rising rate during ammonia combustion increases with pressure, leading to a higher heat release rate. The maximum pressure rising rate at 32 bar is approximately 1.95 times that at 12 bar, with the increase being more significant than the effect of temperature. However, the combustion duration increases slightly at higher pressures due to the larger density of gas in the cylinder. The combustion durations at 15 bar, 22 bar and 32 bar are 26.3 ms, 29.8 ms and 31.2 ms, respectively.

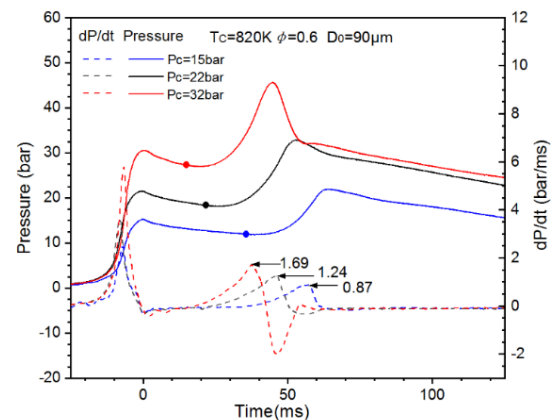


Figure 20. Pressure curves and pressure derivative curves of ammonia-air mixture ignited by diesel droplets under different pressure conditions (corresponding to Figure 19).

Figure 21 shows the relative flame area corresponding to the combustion images. It can be observed that the flame speed slightly decreases

as pressure increases within this pressure range. One of the reasons is that although the reaction rate increases at higher pressures, the increased gas density reduces the diffusion rate. In addition, changes in gas flow properties and viscosity at high pressure increase the resistance to flame propagation, thereby reducing the flame speed. This is consistent with the results of the laminar flame speed study for ammonia in the literature [33].

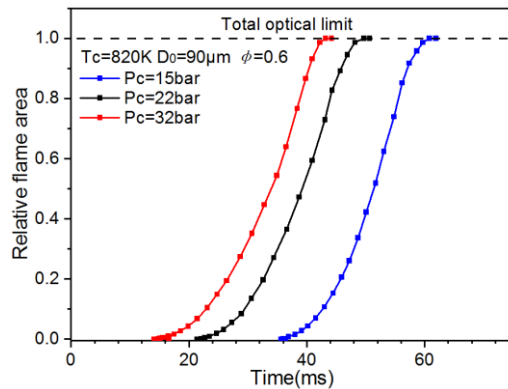


Figure 21. Relative flame area of ammonia-air mixture ignited by diesel droplets under different pressure conditions (corresponding to Figure 19).

3.2.4 Influencing factors of ignition radius

Section 3.1 defines the ignition radius. Figure 22 presents images captured by the long-focus lens, showing the flame propagation of the ambient ammonia-air mixture ignited by the auto-ignition of oil droplets. The shooting frequency was 5000 fps. The red flame of ammonia combustion is not clearly visible due to the significant brightness difference between the ammonia flame and the oil vapor flame, as well as the light source in the experiment. In Figure 22(d), the brightness of the ammonia flame increases, and its flame front edge (indicated by the red dashed line) becomes visible.



Figure 22. Flame propagation images of ammonia-air mixture ignited by the auto-ignition of oil droplets, captured by a long-focus lens ($\phi=0.5$, $T_c=820K$, $P_c=22\text{ bar}$).

The ignition radius is an important parameter in the combustion process of the droplets, which is influenced by various factors [24]. According to experimental results, as shown in Figure 23, the flame radius during droplet combustion decreases with increasing pressure, regardless of the presence and absence of ammonia in the ambient

gas. Due to the transient thermodynamic conditions after the TDC in the RCM, the temperature inside the cylinder also decreases as pressure decreases. Therefore, to account for the influence of pressure on the ignition radius, experimental tests with identical IDTs were selected for comparison, ensuring that both temperature and pressure remained the same throughout the entire process before droplet auto-ignition. The same approach was applied to other control tests.

Furthermore, experiments showed that under the same thermodynamic conditions, changes in droplet diameter had a minimal effect on the ignition radius for droplets with initial diameters ranging from 100 to 150 μm . As a result, the effect of droplet diameter variations was minimized under identical IDT conditions. Additionally, as shown in Figure 24, experiments revealed that temperature had little effect on the ignition radius within the temperature range of 705-885K. As the ammonia equivalence ratio in the background gas increased, the ignition radius showed a significant increase. Figure 25 illustrates the ignition radius of the droplets under different equivalence ratio conditions, with the ignition radius at an equivalence ratio of 1 being approximately 1.7 times that at an equivalence ratio of 0.

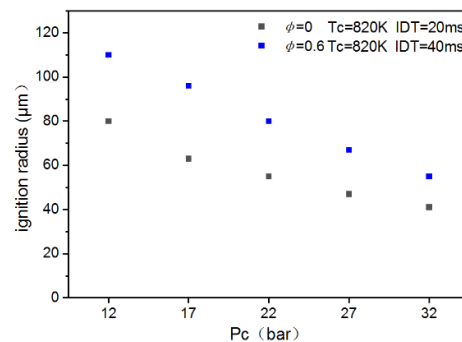


Figure 23. Ignition radius under different pressure conditions.

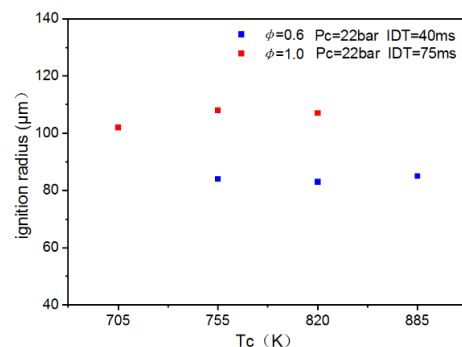


Figure 24. Ignition radius under different temperature conditions.

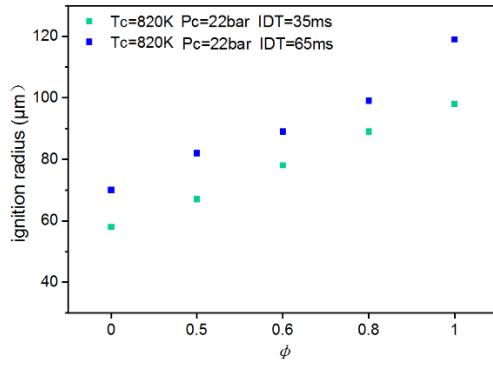


Figure 25. Ignition radius in ammonia mixtures with different equivalence ratios.

3.3 The results of the evaporation experiments

To further investigate the influencing factors of droplet auto-ignition delay time, evaporation experiments were conducted under different conditions. As shown in Figure 26, droplet evaporation can be divided into two periods: the heating period and the evaporation period. In the heating period, the droplet undergoes volumetric expansion as it is heated, and the evaporation rate is relatively low. As the droplet temperature increases, the evaporation rate gradually exceeds the volumetric expansion rate, causing the droplet diameter to decrease. In the evaporation period, the evaporation rate increases significantly, and the droplet begins to evaporate noticeably. Due to heat loss in the RCM, the temperature and pressure inside the cylinder decrease continuously. Some droplets evaporate completely within the measurement time, while others do not fully evaporate by the end of the measurement period (approximately 700 ms in this experiment).

The evaporation period is further divided into two stages. In the first stage, the evaporation rate remains almost constant, which appears to follow the d^2 -law verified under steady-state conditions. However, this behavior involves the interplay of multiple transient factors. Kim et al. [17] proposed that during the expansion process of the RCM, the droplet's evaporation rate is relatively insensitive to changes in the cylinder environment. Therefore, a constant evaporation rate may still be achieved even under the transient conditions in this study.

The evaporation rate constant (Ke) for the droplet in this phase is calculated as follows:

$$Ke = \frac{-d D^2}{dt} \quad (2)$$

where D is the diameter of the droplet and t is the time.

In the second phase, the evaporation rate significantly decreases due to lower temperature and other thermodynamic conditions, and the presence of higher-viscosity residual components. Until the droplet diameter decreases to a very small size, the surface-to-volume ratio of the droplet increases significantly. As a result, heat absorption per unit volume accelerates, and the droplet evaporates rapidly and completely.

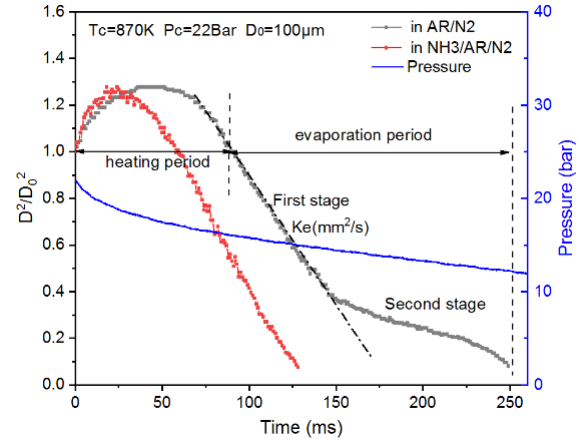


Figure 26. The relative square diameter variation of a 100 μm diesel droplet in ambient gases with and without NH_3 .

Time ATDC (ms)	10.0	30.0	80.0	110.0	150.0	200.0	250.0
(a) In AR/N2 Tc=870K Pc=22bar D ₀ =100 μm							
(b) In NH3/AR/N2 Tc=870K Pc=22bar D ₀ =100 μm							

Figure 27. Visual images of droplet diameter changes of 100 μm diesel droplets evaporated in $\text{NH}_3/\text{AR}/\text{N}_2$ and AR/N_2 gases.

From Figure 26, it can be observed that adding 22% ammonia simultaneously reduces the heating and evaporation times of the droplet. Figure 27 shows a visual comparison of the evaporation of a 100 μm oil droplet under these two atmospheres. A comparison of the evaporation rate constant (Ke) and the droplet lifetime (with the lifetime of incomplete droplet evaporation defined as 670 ms) under different testing conditions is shown in Figure 28. Compared to the AR/N_2 atmosphere, the evaporation rate constant of the droplet is increased, and the heating period is decreased in the $\text{NH}_3/\text{AR}/\text{N}_2$ atmosphere, resulting in a shorter overall droplet lifetime.

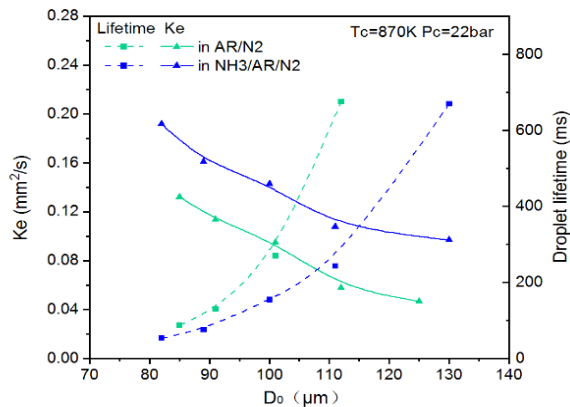


Figure 28. K_e and lifetime of diesel droplets of different initial diameters in ambient gas with or without NH_3 .

Previous studies have shown that properties such as the thermal conductivity, specific heat capacity, and specific enthalpy of environmental gases can all affect the heat transfer from the gas phase to the liquid droplet, thereby influencing the temperature change of the droplet [34]. Additionally, the diffusion rates of diesel in different gases are different, affecting mass transfer and subsequently influencing the evaporation rate. According to available data, under conditions of 725K and 20 bar, the thermal conductivity (in $\text{W}/(\text{m}\cdot\text{K})$) of gases such as NH_3 , N_2 , and AR are 0.093, 0.052, and 0.035, respectively [35]. Among these, ammonia has a significantly higher thermal conductivity than nitrogen and argon, which leads to more efficient heat transfer from the background gas to the oil droplet. This is one of the reasons why the addition of ammonia can accelerate the evaporation rate of diesel.

In addition, the effects of varying the P_c on the droplet evaporation rate and droplet lifetime were investigated in ambient gas with an ammonia equivalence ratio of 1. The results indicate that at 870K, the evaporation rate of the droplet increased with pressure, while the droplet lifetime decreased, with a more pronounced reduction in lifetime at 32 bar. In contrast, the influence of pressure on both the evaporation rate and lifetime became less pronounced at 720K. Similarly, in an ambient gas without ammonia, the effect of pressure on the droplet evaporation rate and lifetime was also less noticeable. This is not further elaborated here. By comparison, temperature had a much greater impact on the droplet evaporation rate and lifetime than pressure in this experiment.

4 CONCLUSIONS

A fundamental experimental study was conducted to investigate the evaporation and auto-ignition characteristics of diesel droplets in air and

ammonia-air mixtures under the operating conditions of an ammonia-diesel dual-fuel engine, using an optical RCM. Several key influencing factors were analyzed. The conclusions are as follows:

- Under the transient thermodynamic conditions of varying temperature and pressure in the RCM, the evaporation period of diesel droplets exhibits a two-stage phenomenon. In the first stage, the evaporation rate is relatively high and follows the d^2 law. Compared to the droplet in AR/N_2 mixture, the droplet in an ammonia-added ambient gas presents a higher evaporation rate. The addition of ammonia gas shortens the heating and evaporation durations, leading to a reduction in the overall droplet lifetime.

- Under the same temperature and pressure conditions, the IDT of diesel droplets increases as the initial droplet diameter increases. Compared to the air atmosphere, the IDT of droplets in ammonia-air ambient gas is longer. Since the droplet IDT is affected by both physical and chemical ignition delays, the rate of increase in IDT becomes less pronounced as the ammonia concentration in the background gas increases. Under the experimental conditions, the droplet IDT is nearly the same at equivalence ratios of 0.8 and 1.0. Furthermore, the droplet IDT decreases with increasing temperature and pressure under all equivalent ratio conditions.

- The ignition radius in oil vapor combustion significantly increases with the decrease in pressure and ammonia equivalence ratio in the ambient gas. However, it is less affected by temperature and droplet diameter variations.

- After the auto-ignition of diesel droplets ignites ammonia gas, the ammonia flame appears as a regular yellow-orange spherical shape propagating outward. As the equivalence ratio increases, the maximum pressure rising rate and the heat release rate during ammonia combustion increase significantly. The combustion duration decreases, and flame speed increases. The maximum pressure rising rate exhibits an exponential increase with the increase in ammonia equivalence ratio. Similarly, the maximum pressure rising rate also increases with temperature and pressure, but their effects are less pronounced than those of the equivalence ratio. Furthermore, flame speed increases with temperature but slightly decreases with pressure. This is due to the different underlying mechanisms of their effects.

5 ACKNOWLEDGMENTS

This work was supported by the Natural Science Foundations of China [grant No. 52471315], [grant

No. 52071061]; and the Research on combustion key technology of Otto-cycle ammonia engine combustion.

6 REFERENCES AND BIBLIOGRAPHY

- [1] <https://www.imo.org/en/OurWork/>.
- [2] Gray N, McDonagh S, O'Shea R, Smyth B, Murphy JD. Decarbonising ships, planes and trucks: An analysis of suitable low-carbon fuels for the maritime, aviation and haulage sectors, *Advances in Applied Energy* 2021;1.
- [3] Wang Y, Cao Q, Liu L, Wu Y, Liu H, Gu Z, et al. A review of low and zero carbon fuel technologies: Achieving ship carbon reduction targets. *Sustainable Energy Technologies and Assessments* 2022;54.
- [4] Chiong M-C, Chong CT, Ng J-H, Mashruk S, Chong WWF, Samiran NA, et al. Advancements of combustion technologies in the ammonia-fuelled engines. *Energy Conversion and Management*, 2021, 244.
- [5] Dimitriou P, Javaid R. A review of ammonia as a compression ignition engine fuel. *International Journal of Hydrogen Energy*, 2020, 45(11):7098-118.
- [6] Kurien C, Mittal M. Review on the production and utilization of green ammonia as an alternate fuel in dual-fuel compression ignition engines. *Energy Conversion and Management*, 2022, 251.
- [7] Gill SS, Chatha GS, Tsolakis A, Golunski SE, York APE. Assessing the effects of partially decarbonising a diesel engine by co-fuelling with dissociated ammonia. *International Journal of Hydrogen Energy*, 2012, 37(7):6074-83.
- [8] Liu L, Wu Y, Wang Y. Numerical investigation on the combustion and emission characteristics of ammonia in a low-speed two-stroke marine engine. *Fuel*, 2022, 314.
- [9] Yousefi A, Guo H, Dev S, Liko B, Lafrance S. Effects of ammonia energy fraction and diesel injection timing on combustion and emissions of an ammonia/diesel dual-fuel engine. *Fuel*, 2022, 314.
- [10] Liu L, Wu Z, Tan F, Wang Y. CFD investigation the combustion characteristic of ammonia in low-speed marine engine under different combustion modes. *Fuel* 2023;351.
- [11] Lewandowski MT, Pasternak M, Haugsvær M, Løvås T. Simulations of ammonia spray evaporation, cooling, mixture formation and combustion in a direct injection compression ignition engine. *International Journal of Hydrogen Energy* 2023.
- [12] Song M, Wang Q, Wang Z, Fang Y, Qu W, Gong Z, et al. Auto-ignition characteristics and chemical reaction mechanism of ammonia/n-heptane mixtures with low n-heptane content. *Fuel* 2024;364.
- [13] Xu L, Xu S, Bai X-S, Repo JA, Hautala S, Hyvönen J. Performance and emission characteristics of an ammonia/diesel dual-fuel marine engine. *Renewable and Sustainable Energy Reviews* 2023;185.
- [14] Niki Y, Nitta Y, Sekiguchi H, Hirata K. Diesel Fuel Multiple Injection Effects on Emission Characteristics of Diesel Engine Mixed Ammonia Gas Into Intake Air. *Journal of Engineering for Gas Turbines and Power* 2019;141(6).
- [15] Wang Z, Yuan B, Huang Y, Cao J, Wang Y, Cheng X. Progress in experimental investigations on evaporation characteristics of a fuel droplet. *Fuel Processing Technology* 2022;231.
- [16] Kim H, Baek SW, Chang D. Auto-Ignition Characteristics of Single n-Heptane Droplet in a Rapid Compression Machine. *Combustion Science and Technology* 2014;186(7):912-27.
- [17] Kim H, Baek SW, Chang D. A single n-heptane droplet behavior in rapid compression machine. *International Journal of Heat and Mass Transfer* 2014; 69:247-55.
- [18] Hashimoto N, Nomura H, Suzuki M, Matsumoto T, Nishida H, Ozawa Y. Evaporation characteristics of a palm methyl ester droplet at high ambient temperatures. *Fuel* 2015; 143:202-10.
- [19] Pang B, Yang G, Liu X, Huang Y, Li W, He Y, et al. Experimental Study of Evaporation Characteristics of Acoustically Levitated Fuel Droplets at High Temperatures. *Energies* 2024;17(1).
- [20] Ju D, Huang L, Zhang K, Ye M, Huang Z, Yi G. Comparison of evaporation rate constants of a single fuel droplet entering subcritical and supercritical environments. *Journal of Molecular Liquids* 2022;347.
- [21] Yi P, Feng L, Jia M, Long W, Tian J. Development of an Improved Multi-Component Vaporization Model for Application in Oxygen-Enriched and EGR Conditions. *Numerical Heat Transfer, Part A: Applications* 2014;66(8):904-27.

- [22] Shahsavan Markadeh R, Ghassemi H. A discrete multicomponent droplet evaporation model; effects of O₂-enrichment, steam injection, and EGR on evaporation of diesel droplet. *Numerical Heat Transfer, Part A: Applications* 2018;73(10):721-42.
- [23] Siddique K, Altarawneh M, Gore J, Westmoreland PR, Dlugogorski BZ. Hydrogen Abstraction from Hydrocarbons by NH₃. *J Phys Chem A* 2017;121(11):2221-31.
- [24] Wang Z, Zhang D, Fang Y, Song M, Gong Z, Feng L. Experimental and numerical investigation of the auto-ignition characteristics of cylinder oil droplets under low-speed two-stroke natural gas engines in-cylinder conditions. *Fuel* 2022;329.
- [25] Wang Z, Zhao H, Liu M, Song M, Fan L, Feng L. Study on the effect and mechanism of EGR on methane/hydrogen pre-ignition caused by cylinder lubricating oil auto-ignition. *Applied Thermal Engineering* 2025;259.
- [26] Gong Z, Hu M, Fang Y, Zhang D, Feng L. Mechanism study of natural gas pre-ignition induced by the auto-ignition of lubricating oil. *Fuel*, 2022,315.
- [27] <https://std.sacinfo.org.cn/gnoc/queryAll>.
- [28] Wang Z, Song M, Zhao H, Lu Y, Gong Z, Feng L. Investigation of the hydrogen pre-ignition induced by the auto-ignition of lubricating oil droplets. *Applied Thermal Engineering* 2025;259.
- [29] Shu B, Vallabhuni SK, He X, Issayev G, Moshhammer K, Farooq A, et al. A shock tube and modeling study on the autoignition properties of ammonia at intermediate temperatures. *Proceedings of the Combustion Institute*, 2019, 37(1):205-11.
- [30] He X, Shu B, Nascimento D, Moshhammer K, Costa M, Fernandes RX. Auto-ignition kinetics of ammonia and ammonia/hydrogen mixtures at intermediate temperatures and high pressures. *Combustion and Flame*, 2019, 206:189-200.
- [31] Ghassemi H, Baek S, Khan Q. Experimental Study on Binary Droplet Evaporation at Elevated Pressure and Temperature. *43rd AIAA Aerospace Sciences Meeting and Exhibit*. 2005.
- [32] Zhang X, Tian J, Cui Z, Xiong S, Yin S, Wang Q, et al. Visualization study on the effects of pre-chamber jet ignition and methane addition on the combustion characteristics of ammonia/air mixtures. *Fuel* 2023;338.
- [33] Zhou Q, Tian J, Zhang X, Cui Z, Ye M, Wang Q, et al. Investigation of the ammonia-methane-air laminar burning characteristics at high temperatures and pressures. *Fuel* 2024;365.
- [34] Yi P, Feng L, Jia M, Long W, Tian J. Development of an Improved Multi-Component Vaporization Model for Application in Oxygen-Enriched and EGR Conditions. *Numerical Heat Transfer, Part A: Applications* 2014;66(8):904-27.
- [35] <https://webbook.nist.gov/chemistry/>.